CHAPTER 182

FRICTION AT THE INTERFACE OF TWO-LAYERED FLOWS

by

Nobuyuki Tamai

Associate Professor
Department of Civil Engineering
University of Tokyo, Tokyo, Japan

ABSTRACT

Viscous perturbed velocity field induced by interfacial waves is solved to the first order in terms of wave amplitude for sharply stratified flows described in a curvilinear coordinate system assuming that the external velocity is uniform and constant along the interface. A new type of formula for the interfacial friction coefficient is proposed based on the theoretical result on viscous dissipation in the boundary layer along the interface. The interfacial friction coefficient is supposed to be inversely proportional to the square root of the product of the Reynolds number of a moving layer and the densimetric Froude number to the fifth. The new formula agrees with observed data better than the best empirical law does especially in the range of large Reynolds number. It is found out, however, that the proportional constant may be affected by stability of the two-layered flow system concerned.

INTRODUCTION

The behavior of saline wedges is directly concerned with the municipal, industrial or agricultural utilization of estuarine waters. The form of the interface and the length of arrested saline wedges have been analyzed by the one-dimensional scheme as the case of varied flows in open channels. However, we have to estimate the value of the interfacial friction coefficient from the bulk hydraulic parameters to perform the prediction in a closed calculation scheme.

One of remarkable flow patterns observed in a two-layered flow system is the generation of interfacial waves and its existence for a relatively wide range of flow conditions. Therefore, the flow regime changes from laminar to turbulent via stable transition zone with interfacial waves. When a whole flow system reaches turbulent condition we have another flow pattern, that is, well mixed estuaries which have density gradient not in vertical direction but in horizontal direction. Although the flow regime in the upper layer(fresh water) is turbulent, the flow regime near the interface is considered in the transition zone due to the suppression of turbulence by the sharp density gradient. In this analysis mixing between two layers is assumed very weak or none. If there exists moderate mixing between two layers, it is supposed that the density distribution may change and the thickness of the mixed zone will develop along the interface. In this case the flow system develops to a different condition from what was assumed initially. Thus we are concerned especially with the case of abrupt interface with stable infinitesimal interfacial waves at the interface as the first approximation of the fresh-salt interface.

Theoretical approaches are classified into two types. One is to consider the energy dissipation of the formation of interfacial waves. This way of approach was initiated by Keulegan(1949) for inviscid fluids. He derived an expression for the interfacial friction coefficient assuming that the dissipation took on the same value as for surface waves in contact with air. He also formulated the additional shearing resistance due to the mixing. Since the liquid crossing the interface is initially at rest and after crossing the interface it acquires the velocity of the current, the current must suffer momentum loss.

Shi-igai(1965) extended the Keulegan's approach to a fresh-salt two-layered flow system. He expressed the flow field by means of the velocity potential. However, interfacial waves were considered to suffer from viscous dissipation. Thus, a virtual shear flow was considered in his analysis. Summarizing the characteristics of interfacial waves, he proposed that the interfacial friction coefficient was inversely proportional to ψ where $\psi=R_eF_d{}^2$. Here R_e is the Reynolds number of a moving layer and F_d is the densimetric Froude number.

Hamada(1966) calculated the dissipation of infinitesimal waves formed on the interface of viscous stratified fluids. He utilized the theoretical results of the Rayleigh-Taylor instability problem. His final result is summarized that the interfacial friction coefficient is inversely proportional to the square root of ψ. However, the theory is built up on the basis of no external flow field, which disagrees with the real situation of salt-water wedges.

Another theoretical approach treats with skin friction and momentum loss due to entrainment of fluid particles from a stationary layer. If we consider the laminar condition for a stationary saline wedge, we can theoretically derive a velocity distribution for both layers and calculate shearing stress of the type of skin friction. In the laminar flow the interfacial friction coefficient is inversely proportional to the Reynolds number of a flowing layer.

Valembois(1963) considered the shearing stress at the interface as the sum of a laminar part and a turbulent part. The turbulent part is expressed by the mixing velocity across the interface. Although he obtained the order of magnitude of these components by utilizing four among forty six experimental data of Lofquist(1960), he did not mention the general behavior of the mixing velocity any further.

Recently Pedersen(1972) investigated the mechanism of entrainment in two-layer stratified flows. With the use of the momentum and work energy equations, both with respect to the net entrainment, the interfacial friction coefficient is found to be equal to the non-dimensional entrainment velocity. The details of the entrainment velocity, however, remained vague with respect to hydraulic parameters of a flowing layer since the interfacial friction coefficient appeared to be a minor objective in his paper.

As was briefly reviewed there are several components which contribute to the friction at the interface of a stratified flow. Referring to the proposed functional relationship it is said that when the Reynolds number is very large and the stratification is stable, which is encountered in saline wedges in estuaries, the magnitude of laminar friction is much smaller than that of the friction due to interfacial wave formation. In addition, as long as we consider a two-layered flow system the mixing between two layers remains weak. Therefore, it is supposed that the friction due to the mixing does not play a dominant role in sharply stratified flows with which we are concerned in this paper. The objective of this paper is to construct a more advanced theory on the interfacial friction under the existence of interfacial waves. Main flow is divided into two parts, that is, an inviscid part and a viscous perturbed part so as to improve previous theories. Then, boundary layer along the wavy interface is analyzed and the interfacial friction coefficient is derived from viscous dissipation in the boundary layer.

THEORETICAL CONSIDERATIONS

The definition sketch of a two-dimensional two-layered flow system is given in Fig. 1. The coordinate system (x,y) is a moving frame with the celerity of interfacial waves, c. We have stable infinitesimal interfacial waves at the interface. The velocity distribution in the upper layer is assumed uniform. This is because the flow of the upper layer is considered turbulent, though the flow regime near the interface is in the transition due to the suppression of turbulence by the density difference. Since the relative importance of skin friction with the resistance due to interfacial waves diminishes as the Reynolds number becomes high, the velocity distribution is not essential in this analysis. The salt-water layer is assumed stationary. If we consider this motion as a relative motion, the situation is general.

The coordinate system (x,y) is transformed into a curvilinear coordinate system (ξ,η) by utilizing a conformal mapping.

$$\zeta = \xi + i\eta = z - ia\, e^{ikz} \tag{1}$$

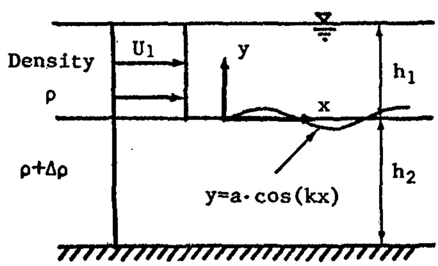

Fig. 1. Definition sketch of a two-layered flow

where $z=x+iy$, a is the amplitude of an infinitesimal interfacial wave, and k is the wave number. From Eq. (1) we obtain

$$\xi = x + a\, e^{-ky} \sin kx, \qquad \eta = y - a\, e^{-ky} \cos kx \tag{2}$$

Jacobian of the transformation is calculated as

$$J = 1 + 2ak\, e^{-ky} \cos kx + O(a^2) \tag{3}$$

The interface is expressed by $\eta=0$ if we neglect the effect of the order of a^2.

The vorticity transport equation for a steady motion is expressed by

$$\boldsymbol{u} \cdot \nabla \boldsymbol{\omega} - \boldsymbol{\omega} \cdot \nabla \boldsymbol{u} = \nu \nabla^2 \boldsymbol{\omega} - \nabla(1/\rho)_{\wedge} \nabla p \tag{4}$$

where $\boldsymbol{u}$ and $\boldsymbol{\omega}$ are velocity and vorticity vectors, respectively, ν the kinetic viscosity of the fluid, ρ the density of the fluid, p the pressure, ∇ a gradient operator, $\cdot$ inner product, and $\wedge$ vector product. Equation of continuity for an incompressible fluid is explained by

$$\nabla \cdot \boldsymbol{u} = 0 \tag{5}$$

Equation (5) is an exact expression for the equation of continuity even in the case of slight density variation due to a solute and is a passable expression to the first order approximation under the density variation caused by both temperature and concentration(Yih,1965). The equation of continuity in the curvilinear coordinate transformed by Eq. (1) is

$$J \left\{ \frac{\partial}{\partial \xi}(J^{-1/2}u) + \frac{\partial}{\partial \eta}(J^{-1/2}v) \right\} = 0 \tag{6}$$

where u and v are ξ and η components of velocity, respectively. Equation (6) is satisfied by the stream function, X, defined by

$$u = J^{1/2} \frac{\partial X}{\partial \eta}, \qquad v = -J^{1/2} \frac{\partial X}{\partial \xi} \tag{7}$$

In a two-dimensional problem vorticity has just one component perpendicular to ξ-η plane. Therefore we can treat vorticity as a scalar denoting $|\boldsymbol{\omega}| = \omega$. Further, the second term of the left-hand side of Eq. (4) vanishes in case of a two-dimensional problem. Because a sharply stratified flow is considered in this analysis, density gradient and pressure gradient are parallel each other. Therefore, the second term of the right-hand side of Eq. (4) also vanishes in this case. Equation (4) is thus rewritten as in Eq. (8).

$$- J^{1/2} \frac{\partial X}{\partial \xi} \cdot J^{1/2} \frac{\partial \omega}{\partial \eta} + J^{1/2} \frac{\partial X}{\partial \eta} \cdot J^{1/2} \frac{\partial \omega}{\partial \xi} = \nu J D^2 \omega \tag{8}$$

where $\omega = -JD^2 X$ and $D^2 = \partial^2/\partial\xi^2 + \partial^2/\partial\eta^2$.

Now perturbation method is applied to solve Eq. (8). Stream function defined in Eq. (7) is expanded in power series as shown in the next equation.

$$X = X_0 + \varepsilon X_1 + \varepsilon^2 X_2 + \cdots\cdots \tag{9}$$

where the suffix of X stands for the order of a perturbed representation and $\varepsilon = ak$. We assume the external flow is inviscid. Therefore, X_0 is obtained by the inviscid theory. X_1 is composed of a wave component, X_{1_w}, which is also calculated by the inviscid theory and a viscous component, X_{1_v}. Substitution of Eq. (9) into the definition of vorticity yields

$$\begin{aligned} \omega &= -JD^2X = \omega_0 + \varepsilon\omega_1 + \varepsilon^2\omega_2 + \cdots\cdots \\ &= -\{ 1 + 2\varepsilon e^{-k\eta} \cos k\xi + O(\varepsilon^2) \}\cdot(D^2X_0 + \varepsilon D^2X_1 + \varepsilon^2 D^2 X_2 +\cdots) \\ &= -\varepsilon D^2X_1 - \varepsilon^2(D^2X_2 + 2e^{-k\eta} \cos k\xi\cdot D^2X_1) + O(\varepsilon^3) \end{aligned} \tag{10}$$

Since X_0 is derived from the inviscid theory, it provides irrotational motion. Thus the perturbed expression for vorticity begins with the first order in terms of ε.

The equation in ε is obtained as follows by substitution of Eqs. (9) and (10) into Eq. (8).

$$-\frac{\partial X_0}{\partial\xi}\frac{\partial}{\partial\eta} D^2X_1 + \frac{\partial X_0}{\partial\eta}\frac{\partial}{\partial\xi} D^2X_1 = \nu D^2(D^2X_1) \tag{11}$$

According to the Kelvin-Helmholtz problem, the inviscid solution of the stream function is given by

$$\begin{aligned} \Psi &= (U_1-c)y + \frac{(U_1-c)a}{\sinh kh_1} \sinh k(y-h_1) \cos kx \\ &= (U_1-c)\eta + (U_1-c)ae^{-k\eta} \cos k\xi + \frac{(U_1-c)a}{\sinh kh_1}\sinh k(\eta-h_1) \cos k\xi \\ &\quad + O(a^2) \end{aligned}$$

where Ψ is the stream function, U_1 the velocity of the upper layer, and h_1 the depth of the upper layer. The stream function defined by Eq. (9) is thus obtained up to the order of ε as

$$\left\{ \begin{aligned} X_0 &= (U_1-c)\eta \\ X_1 &= \frac{1}{k}(U_1-c)e^{-k\eta} \cos k\xi + \frac{U_1-c}{k \sinh kh_1} \sinh k(\eta-h_1) \cos k\xi + X_{1_v} \\ &= X_{1_w} + X_{1_v} \end{aligned} \right. \tag{12}$$

Following Eq. (12) we obtain $\partial X_0/\partial\xi = 0$. Therefore, we can simplify Eq. (11) further as

$$(U_1-c)\frac{\partial\omega_1}{\partial\xi} = \nu D^2\omega_1 \tag{13}$$

In addition length scale along the interface is considered much larger than that of the direction perpendicular to the interface. Hence $\partial/\partial\xi \ll \partial/\partial\eta$ and $\partial^2/\partial\xi^2 \ll \partial^2/\partial\eta^2$ may hold to reduce the governing equation as in the following expression.

$$(U_1-c)\frac{\partial\omega_1}{\partial\xi} = \nu\frac{\partial^2\omega_1}{\partial\eta^2} \tag{14}$$

where $\omega_1 = -\partial u_1/\partial\eta$. Here u_1 is the first order component of perturbed velocity.

Now the velocity component along the interface is developed in power series through Eq. (7).

$$\begin{aligned} u &= u_0 + \varepsilon u_1 + \varepsilon^2 u_2 + \cdots\cdots \\ &= \frac{\partial X_0}{\partial\eta} + \varepsilon\{\frac{\partial X_1}{\partial\eta} + (U_1-c)e^{-k\eta}\cos k\xi\} + O(\varepsilon^2) \end{aligned} \tag{15}$$

Boundary conditions under which Eq. (14) is to be solved are determined as follows. As was previously mentioned the interface is expressed by $\eta=0$ to the order of ε. Fundamental scheme on the velocity of this paper is that we allow velocity gap in the external flow but we impose no-slip condition for perturbation velocities. Therefore, we have

$$u_1 = 0 \quad \text{at} \quad \eta = 0, \qquad u_1 = \frac{\partial X_{1_w}}{\partial\eta} \quad \text{at} \quad \eta = \infty$$

The second condition shows that viscous effect vanishes as the distance from the interface increases. If we denote wavy and viscous parts in the perturbed velocity separately, we obtain the following expression from Eqs. $(12)_3$ and $(15)_2$.

$$\left\{\begin{aligned} &u_1 = u_{1_w} + u_{1_v} + (U_1-c)e^{-k\eta}\cos k\xi \\ &u_{1_w} = \partial X_{1_w}/\partial\eta, \qquad u_{1_v} = \partial X_{1_v}/\partial\eta \end{aligned}\right. \tag{16}$$

Thus we obtain the boundary conditions in terms of the first order viscous perturbed velocity, u_{1_v}.

$$\left\{\begin{aligned} &u_{1_v} = (U_1-c)\coth kh_1 \cos k\xi \qquad \text{at} \quad \eta = 0 \\ &u_{1_v} = 0 \qquad\qquad\qquad\qquad\qquad\quad \text{at} \quad \eta = \infty \end{aligned}\right. \tag{17}$$

The governing equation (14) is again rewritten in terms of u_{1_v}.

$$(U_1-c)\frac{\partial^2 u_1}{\partial\xi\partial\eta} = \nu\frac{\partial^3 u_1}{\partial\eta^3} \tag{18}$$

Integration with respect to η produces Eq. (19).

$$(U_1-c)\frac{\partial u_1}{\partial\xi} = \nu\frac{\partial^2 u_1}{\partial\eta^2} + H(\xi) \tag{19}$$

Integration constant $H(\xi)$ is considered pressure gradient referring to a momentum equation.

The solution to Eq. (19) is obtained with boundary conditions of Eq. (17) for the case of $H(\xi)$ equals zero, which represents constant external velocity. This is the case that the interface is parallel to the water surface and would be the first approximation even for the case of slightly inclined interface.

$$u_{1_v} = (c-U_1)\coth kh_1 \; e^{-\beta\eta} \cos(k\xi+\beta\eta) \tag{20}$$

where

$$\beta = \sqrt{(c-U_1)k/2\nu} \tag{21}$$

Vorticity is thus calculated up to the first order.

$$\begin{aligned}\omega &= \varepsilon\omega_1 = -\varepsilon\partial u_1/\partial\eta \\ &= \beta(c-U_1)ak \coth kh_1 \; e^{-\beta\eta}\{\cos(k\xi+\beta\eta) + \sin(k\xi+\beta\eta)\}\end{aligned} \tag{22}$$

In order to obtain a real value for β in Eq. (21), the condition $c \geqq U_1$ must be hold. The interfacial wave propagating downstream satisfies this condition. A more detailed description will be given as follows. Let us denote $\Delta\rho=\rho_2-\rho_1$ and $g'\equiv g\cdot\Delta\rho/\rho_1$, where $\Delta\rho$ is the density difference between upper and lower layers and g is the acceleration of gravity. For the case of a stationary lower layer and of a slight density difference, which is treated in this paper, the condition $c \geqq U_1$ can be rewritten on use of the inviscid theory as

$$g' \geqq kU_1^2 \coth kh_2 \tag{23}$$

where h_2 is the thickness of the lower layer. For long waves we can approximately express $\coth kh_2=1/kh_2$. Thus Eq. (23) reduces to

$$(1/F_d^2)(h_2/h_1) \geqq 1 \tag{24}$$

where

$$F_d = \frac{U_1}{\sqrt{\frac{\Delta\rho}{\rho_1} gh_1}} \tag{25}$$

is the densimetric Froude number. The value of F_d is less than unity in density currents like as saline wedges. Therefore, the condition of Eq.(24) is ordinarily satisfied unless the thickness of the lower layer is extremely small. For deep water waves we can put approximately $\coth kh_2=1$. Then we obtain the relationship for the wave length λ

$$\lambda \geqq 2\pi h_1\cdot F_d^2 \tag{26}$$

Equation (26) shows that interfacial waves whose wave length is shorter than that given by Eq. (26) are unstable. Since we can expect to have real values for β for usual hydraulic conditions as shown in Eqs. (24) and (26), we can accept Eq. (22) as a basis for further investigation.

Viscous energy dissipation is generated in the boundary layer, the thickness of which is the order of $1/\beta$, along the interface. In this analysis the boundary layer is only considered along the upper surface of the interface. This may be acceptable under the assumptions adopted in this analysis that the lower layer is stationary, the density profile is discontinuous at the interface and the amplitude of interfacial waves is infinitesimal. The mean energy dissipation per unit area is given by

$$\dot{E} = -\mu \int_0^\delta \overline{\omega^2} \, d\eta \tag{27}$$

where δ is the thickness of the boundary layer and overbar denotes the average over a wave length. Substituting Eq. (22) into Eq. (27) we obtain

$$\dot{E} = -(1/2)\mu\beta(c-U_1)^2 a^2 k^2 \coth^2 kh_1 \tag{28}$$

where the outer edge of the boundary layer is approximated by $\eta=\infty$.

This energy dissipation must be fed by the mean flow of the upper layer. The resistance stress to the upper layer, τ, is thus obtained by dividing the rate of energy dissipation by the mean flow velocity of the upper layer and turning the sign following the definition of the resistance stress.

$$\tau = -\dot{E}/U_1 \tag{29}$$

Interfacial friction coefficient, f_i, defined by

$$\tau = (1/2)\, f_i \rho U_1{}^2 \tag{30}$$

is then obtained on use of Eqs. (28),(29), and (30).

$$f_i = \frac{1}{\sqrt{2}} R_e{}^{-1/2}\left(\frac{c}{U_1}-1\right)^{5/2}(kh_1)^{1/2} a^2 k^2 \coth^2 kh_1 \tag{31}$$

where

$$R_e = \frac{U_1 h_1}{\nu} \tag{32}$$

is the Reynolds number of the upper layer. It is noted that in this analysis the energy dissipation is not caused by the maintenance of interfacial waves but by the viscous perturbed velocity field which is induced by the presence of interfacial waves.

It is found out that the interfacial friction coefficient is inversely proportional to the square root of the Reynolds number of the moving layer. In order to study the dependence on the densimetric Froude number we have to specify the magnitude of interfacial wave celerity which is obtained by the inviscid theory.

$$c = \frac{U_1 \coth kh_1 + \{g'(\coth kh_1 + \coth kh_2)/k - U_1{}^2 \coth kh_1 \coth kh_2\}^{1/2}}{\coth kh_1 + \coth kh_2} \tag{33}$$

For a real value of β only plus sign of the square root is considered. This expression can be simplified in two extreme cases of long waves and deep water waves. Further analysis on the frictional coefficient is developed for these cases.

(a) *The case of long waves*: We can put approximately $\coth kh_1 = 1/kh_1$, and $\coth kh_2 = 1/kh_2$. From Eq. (33) we obtain

$$\frac{c}{U_1} = \frac{h_2 + \{F_d{}^{-2} h_2(h_1+h_2) - h_1 h_2\}^{1/2}}{h_1 + h_2}$$

(i) $h_2 >> h_1$

In this case Eq. (31) reduces to

$$f_i = 0.707\ (R_e F_d{}^5)^{-1/2}\ (kh_1)^{1/2}\ a^2 k^2 \coth^2 kh_1 \tag{34}$$

(ii) $h_2 \approx h_1$

In this case Eq. (31) is rewritten as

$$f_i = 0.125\ R_e^{-1/2}\ (\sqrt{2F_d^{-2}-1} - 1)^{5/2}(kh_1)^{1/2}\ a^2k^2\ \coth^2 kh_1 \qquad (35)$$

For very small values of F_d, Eq. (35) reduces to the same type of formula as Eq. (34).

$$f_i = 0.297\ (R_eF_d^5)^{-1/2}\ (kh_1)^{1/2}\ a^2k^2\ \coth^2 kh_1 \qquad (36)$$

(b) *The case of deep water waves*: In this case coth kh_1 and coth kh_2 are approximated to be unity. From Eq.(33) we obtain

$$c/U_1 = (1/2)\{\ 1 + \sqrt{\lambda/(\pi h_1F_d^2) - 1}\ \}$$

Substitution of the above expression into Eq. (31) yields

$$f_i = 0.125\ R_e^{-1/2}\ \{\sqrt{\lambda/(\pi h_1F_d^2)-1}\ -1\}^{5/2}(kh_1)^{1/2}a^2k^2\ \coth^2 kh_1 \quad (37)$$

A few remarks on Eq. (37) are added. For the shortest waves that satisfies Eq. (26) f_i reduces to zero. In that case the celerity of the interfacial wave is identical to the mean flow velocity. Thus the upper layer does not suffer from the energy dissipation. The longest wave that satisfies the deep water condition is written as $\lambda=2h_1$. For this wave we can simplify Eq. (37). If we assume the densimetric Froude number F_d is much smaller than unity, Eq. (37) gives the relationship $f_i \propto (R_eF_d^5)^{-1/2}$.

COMPARISON WITH MEASURED DATA AND DISCUSSION

There have been several experimental works and field observations on saline wedges. Reported data of the interfacial friction coefficient are rearranged on the light of a newly developed formula. Referring to Eqs. (34), (35) and (37), the frictional coefficient depends on the wave characteristics even in specified cases. However, none has been reported explicitly about the wave length, the amplitude, and the celerity of interfacial waves. Therefore whichever formula we choose, certain magnitude of scattering of data around the estimated relationship will be inevitable.

Previous formulae claim the type of relationship

$$f_i = \alpha\ \psi^{-n} \qquad (38)$$

where α and n are constants and $\psi = R_eF_d^2$. Because no observational result explains the amplitude and the wave length of interfacial waves as mentioned above, we have to simplify Eq. (31) in order to compare the theoretical result with reported data. The newly derived formula is approximated as in Eq. (39) excluding the effect of the characteristics of interfacial waves.

$$f_i = m\ (R_eF_d^5)^{-1/2} \qquad (39)$$

where m is a proportional constant. This type of formula is chosen in connection with Eqs. (34), (35) and (37). Note that for very small F_d Eqs. (35) and (37) reduces to the same type of relation as Eq. (34).

The observed data are shown in Fig. 2 in the relationship between f_i and $R_eF_d^5$. Detailed values of f_i, R_e, and F_d of each data are listed in Table 1. A full line in Fig. 2 shows Eq. (39) in which m=0.085. The author's experiment(Tamai,1964) was performed in a flume 15cm wide and 420 cm long and interfacial profiles of stationary saline wedges were recorded for a bottom slope of 1.27/100. Values of the interfacial friction coefficient were selected to produce the best fit interfacial profile by the numerical integration of a one-dimensional open channel equation for two-layered flows. The determined interfacial friction coefficient is thus considered the average value over the interface. The Reynolds number of the upper layer remains constant even for an inclined interface because of the constant discharge per unit width. The representative depth of the upper layer to calculate F_d is chosen at the mid-point of intruded saline wedges.

Lofquist(1960) performed his experiment in a horizontal flume 23.3cm wide and 30m long. In his experiment a heavier salt-water layer moved underneath a stationary fresh-water layer. Mean shear stress with respect to width at the interface were calculated from the slope of the interface, bed shear stress, and velocity gradient. Although friction coefficient is given with respect to the maximum velocity in the paper, the conversion to the definition of Eq. (30) is available utilizing the listed quantities.

Nakamura and Abe(1970) observed the behavior of a saline wedge in the Kuzuryu River. Values of the interfacial friction coefficient were calculated by the equation

$$f_i = 2\, F_d^{-2} \frac{h_1}{h_1+h_2} \left\{-(1-F_d^2)\frac{\Delta h_1}{\Delta x} + \frac{U_1^2}{(\Delta\rho/\rho_1)gB}\frac{\Delta B}{\Delta x}\right\} \tag{40}$$

Here we assume a stationary lower layer and B is the width of a channel. Symbol Δ explains finite difference in the marked quantities and x is a coordinate axis taken to the direction of fresh-water flow. It is noted that the resulted interfacial friction coefficient through Eq. (40) is considered a local value at a certain position in two-layered flows.

Suga and Takahashi(1971) performed a field observation in the Tone River and experiments in two flumes. One is 80cm wide and 100m long and the other is 30cm wide and 30m long. Values of the interfacial friction coefficient were computed by Eq. (40). Other data reported previously cannot be rearranged in Fig. 2 because the data are tabulated only with the value of ψ which is the sole parameter in the existing formula, Eq.(38). Thus the value of R_e and F_d cannot be obtained separately.

In f_i versus ψ diagram the best fit empirical formula was the case that α=0.2 and n=1/2 in Eq. (38). But the value of n to explain the trend of the data measured in the Tone River that is one of the largest rivers in Japan is about 6/5. Therefore, the empirical formula fails to explain the behavior of the interfacial friction coefficient in the largest range of ψ. The trend of the data obtained in the Tone River which are indicated in solid circles in Fig. 2 seems to follow a line

$$f_i = 0.025\ (R_e F_d^5)^{-1/2} \tag{41}$$

The trend agrees with what the new formula, Eq. (39), predicts, though the magnitude of coefficient is different from other groups of data.

Generally speaking scattering around the solid line

$$f_i = 0.085\ (R_e F_d^5)^{-1/2} \tag{42}$$

in Fig. 2 is smaller than that shown in f_i versus ψ diagram by previously proposed formulae. The data reported by Lofquist(1960) illustrated by sol-

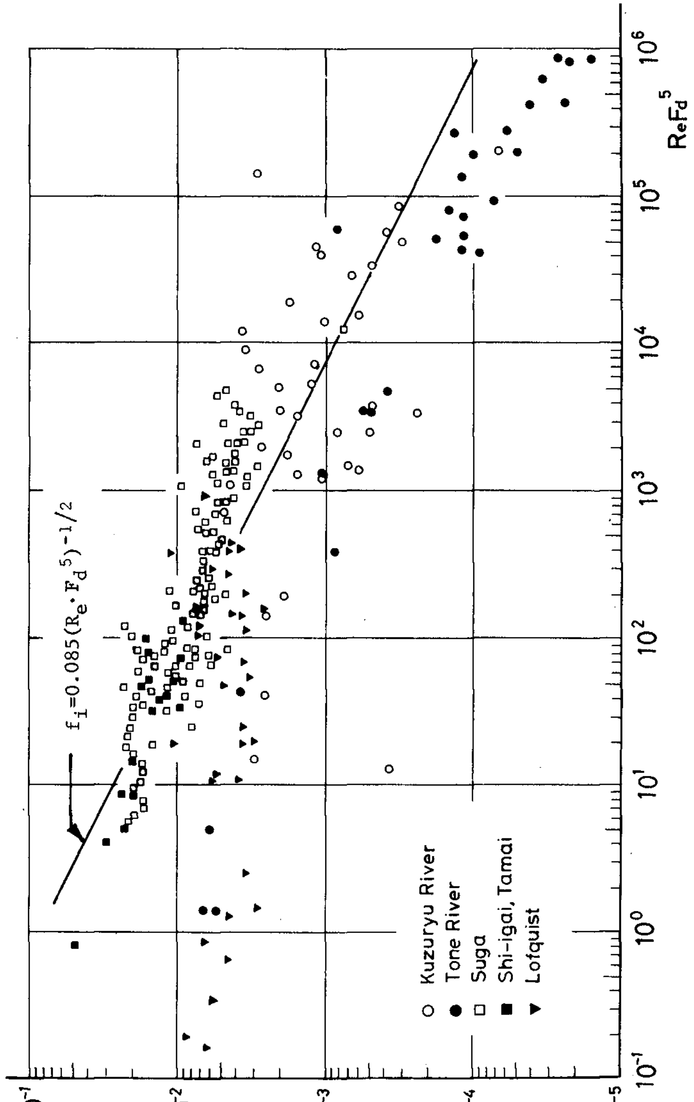

Fig. 2. Interfacial friction coefficient vs. $R_eF_d^5$

id reversed triangles in Fig. 2 behave differently from others. Previously only four cases in forty six of Lofquist's experimantal results were reported by Valembois(1963). Present analysis revealed that the different relationship held for a set of all forty six data. The magnitude of the interfacial friction coefficient remains almost unchanged regardless of the value of the abscissa. This is partly because Lofquist performed his experiments with a moving denser fluid while a lighter upper layer remained stationary and therefore the results might be affected more strongly by bottom shear. Although the trend is not so clear as Lofquist's data, the data obtained in the Kuzuryu River expressed by open circles in Fig. 2 shows nearly the same feature.

The measured data follow the trend explained by Eq. (42) on the whole. As mentioned above, however, there is a more appropriate formula like Eq. (41) for a special group of data. The variety of the magnitude of coefficients of the derived formulae is discussed from the standpoint of the stability of a two-layered flow system. Equation (43) is an interpretation of the reciprocal of the Keulegan number by Turner(1973).

$$\theta = \left(\frac{\rho U_1^{\,2}}{\Delta\rho g\delta} \right) \left(\frac{U_1 x}{\nu} \right)^{1/2} \tag{43}$$

Here δ denotes the thickness of the boundary layer and x is the length of contact of two layers along the interface. In field observation like the case of the Tone River the length of the contact of interface measured from the saline wedge toe may be much larger than that encountered in experimental flumes. Thus the Keulegan number observed in natural streams is expected much smaller than the critical value if it exists at all. Therefore, the stability of field data may be higher than that obtained in experiments.

The amplitude of the lowest internal mode obtained by Phillips(1969) is expressed for $n \ll N_m$ by

$$a^2k^2 = \left(\frac{N_m}{n} \right)^{-2} J^{-1}$$

where n is the frequency of an internal wave mode, N_m the maximum Brunt-Väisälä frequency ($N \equiv \{-(g/\rho)(\partial\rho/\partial y)\}^{1/2}$), J the local Richardson number. Substitution of this expression into the derived relationship, Eq. (34), yields

$$f_i = 0.707\ (R_e F_d^{\,5})^{-1/2}\ (kh_1)^{-3/2}\ (n/N_m)^2\ J^{-1} \tag{44}$$

This suggests that the higher the stability of a two-layered flow system is, the lesser the magnitude of the interfacial friction coefficient will be, which explains the feature of the observed data qualitatively.

One more comment on the field data is added. Values of the interfacial friction coefficient were calculated by Eq. (40) which was applicable only to steady motions. Since tidal motion affects the behavior of saline wedges continuously, we would have measured various hydraulic quantities under unsteady conditions in reality. This discrepancy from the assumed condition may explain the scattering of field data.

CONCLUSIONS

An advanced theory on the interfacial friction of sharply stratified two-layered flows is developed. Because the magnitude of laminar friction is much smaller than that of the friction due to interfacial wave formation in case of the large Reynolds number, the theory is formulated under the existence of interfacial waves. The solution to a governing equation is obtained to the first order in terms of wave amplitude by perturbation method. No-slip condition is imposed for the first order solution and external flow velocity is assumed uniform and constant. In this theory it is considered that the energy dissipation is caused by the viscous perturbation velocity field which is induced by the presence of interfacial waves.

Based on the theoretical result a new type of formula for the interfacial friction coefficient is proposed discarding the detailed properties of interfacial waves which have not been reported in available form. It is said that the agreement between the proposed relationship, that is, f_i is proportional to $(R_eF_d{}^5)^{-1/2}$, and the observed data is better than that demonstrated by the best empirical formula, $f_i \propto (R_eF_d{}^2)^{-1/2}$. Scattering of data may be attributed to the stability of two-layered flows. It is pointed out that the proportional constant in the new formula decreases its magnitude as the stability increases.

This study has explained the hydrodynamic feature of the interfacial friction coefficient under the existence of interfacial waves with no mixing between two layers. In order to determine the more detailed feature of the derived expression, it is still needed to obtain reliable data from which we can specify the interfacial wave characteristics and to develop a more refined theory which can take account of the effect of viscosity even in the zeroth order principal velocity or of the accelaration of the external flow.

ACKNOWLEDGMENTS

The author wishes to express his gratitude to Professor Tosio Iwasaki at Tohoku University for his promotion and valuable suggestions to this study. Cordial assistance offered by Mr. Hiroshi Nakamura of Central Research Institute of Electric Power Industry and by Mr. Kyozo Suga of Public Works Research Institute is also appreciated. Rearrangement of field data would not have been performed without their cooperation of providing the details of their observation data.

REFERENCES

Hamada, T.(1966) "On density currents(1)",Proc. 13th Japanese Conf. on Coastal Eng., JSCE, 259-262(in Japanese).

Keulegan, G.H.(1949) "Interfacial instability and mixing in stratified flows", J. of Research, Nat. Bureau of Stands., Vol.43, 487-500.

Lofquist, K.(1960) "Flow and stress near an interface between stratified liquids", The Physics of Fluids, Vol.3, 158-175.

Nakamura, H. and N. Abe(1970) "Salt-water wedge in the Kuzuryu River estuary", Rept. of 2nd Tech. Lab., Central Res. Inst. of Electric Power Industry, No.70519(in Japanese).

Pedersen, F.B.(1972) "Gradually varying two-layer stratified flow", J. Hy. Div.,Proc. ASCE, Vol.98, HY-1, 257-268.

Phillips, O.M.(1969) "The Dynamics of the Upper Ocean", Cambridge Univ. Press, 168.
Shi-igai, H.(1965) "On the resistance coefficient at the interface between salt and fresh water", Trans. JSCE, No.123, 27-31.
Suga, K. and A. Takahashi(1971) "A study on the salt-water wedge by a large flume", Proc. 26th Annual Meeting, JSCE, Sec. II, 137-140 (in Japanese).
Tamai, N.(1964) "An experimental study on saline wedges", Graduation Thesis, Dept. of Civil Eng., Univ. of Tokyo, 95pp. (in Japanese).
Turner, J.S.(1973) "Buoyancy Effects in Fluids", Cambridge Univ. Press, 108.
Valembois, J.(1963) "Courants de densité: tension tangentielle à l'interface, Essai d'interprétation des résultas de Lofquist", Bulletin du Centre de Recherches et d'Essais de Chatou, No.5, 37-40.
Yih, C.-S.(1965) "Dynamics of Nonhomogeneous Fluids", Macmillan, 152-154.

Table 1 - Interfacial Friction Coefficient

$\varepsilon = \Delta\rho/\rho_1$

Experiment, Reporter: Tamai — c.g.s. unit

Run	h_1	U_1	$\nu \cdot 10^2$	$\varepsilon \cdot 10^2$	$R_e \cdot 10^{-3}$	F_d	$f_i \cdot 10^2$
1	7.1	4.47	1.240	1.05	2.56	0.523	1.67
2	7.2	4.26	1.275	1.00	2.42	0.508	1.60
3	7.1	4.21	1.275	1.00	2.35	0.505	1.45
4	7.2	3.99	1.275	1.00	2.26	0.474	1.58
5	7.1	3.90	1.275	1.00	2.18	0.468	1.58
6	7.1	3.76	1.275	1.00	2.10	0.451	1.34
7	6.6	3.89	1.240	1.05	2.07	0.472	1.74
8	5.6	4.64	1.312	1.15	1.99	0.584	0.93
9	5.7	4.23	1.312	1.15	1.84	0.528	0.96
10	5.7	3.98	1.312	1.15	1.73	0.498	1.07
11	5.7	3.84	1.312	1.15	1.67	0.480	1.20
12	5.7	3.51	1.312	1.05	1.61	0.459	1.50
13	5.5	3.69	1.312	1.15	1.55	0.470	0.98
14	6.7	2.87	1.275	1.00	1.51	0.354	2.00
15	6.8	2.65	1.275	1.00	1.42	0.324	2.32
16	5.5	2.91	1.210	0.95	1.32	0.407	2.08
17	5.2	2.65	1.240	0.95	1.11	0.381	2.46
18	5.1	2.33	1.275	0.95	0.934	0.338	3.18
19	4.7	1.70	1.275	0.90	0.630	0.264	4.82

Experiment, Reporter: Lofquist — c.g.s. unit

Run	h_1	U_1	$\nu \cdot 10^2$	$\varepsilon \cdot 10^2$	$R_e \cdot 10^{-3}$	F_d	$f_i \cdot 10^3$
3	7.13	3.54	0.952	1.18	2.65	0.375	10.7
4	7.02	4.83	0.956	1.11	3.55	0.538	7.44
6	7.27	5.41	0.928	1.07	4.24	0.618	11.3
7	6.47	1.55	0.928	1.19	1.08	0.180	8.95
8	7.10	2.38	0.904	1.19	1.87	0.204	4.58
9	7.19	3.42	0.900	1.20	2.73	0.371	4.67
10	7.21	4.59	0.902	1.17	3.67	0.504	7.20
11	7.47	4.96	0.889	1.13	4.17	0.545	7.12
12	6.92	2.52	0.842	2.08	2.07	0.211	6.77
13	6.84	3.86	0.835	2.09	3.16	0.326	3.90
14	6.93	4.98	0.828	2.08	4.17	0.408	4.99
15	7.22	5.70	0.849	2.10	4.85	0.466	7.31
16	7.25	6.72	0.844	2.04	5.77	0.555	5.47
17	6.92	2.49	0.870	3.00	1.98	0.173	5.77
18	7.13	4.64	0.855	3.02	3.87	0.316	5.58
19	6.96	6.20	0.872	2.89	4.95	0.438	4.29
20	7.11	6.94	0.864	2.92	5.71	0.483	4.58
21	7.27	7.71	0.860	2.88	6.52	0.535	6.01
22	7.37	8.27	0.856	2.86	7.12	0.570	6.75
23	6.90	2.51	0.875	3.92	1.98	0.153	6.35
24	6.90	5.04	0.857	3.97	4.06	0.305	5.92
25	7.10	7.05	0.849	4.01	5.90	0.418	5.55

Table 1 (continued)

Run	h_1	U_1	$\nu \cdot 10^2$	$\varepsilon \cdot 10^2$	$R_e \cdot 10^{-3}$	F_d	$f_i \cdot 10^3$
26	7.15	8.08	0.869	4.18	6.65	0.468	4.38
27	7.25	8.75	0.863	3.94	7.35	0.517	4.61
28	7.17	9.03	0.853	3.75	7.59	0.551	4.67
29	7.51	4.01	0.896	4.80	3.36	0.210	4.47
30	7.01	7.20	0.881	4.73	5.73	0.394	3.32
31	6.97	8.50	0.867	4.65	6.83	0.471	2.68
32	7.19	9.05	0.880	4.72	7.39	0.490	3.66
33	7.14	10.01	0.873	4.60	8.19	0.552	3.56
34	7.32	10.20	0.872	4.68	8.56	0.550	4.57
35	7.06	4.74	0.920	5.74	3.64	0.232	3.34
36	7.09	6.95	0.924	5.61	5.33	0.346	3.69
37	7.04	8.31	0.905	5.67	6.46	0.404	3.63
38	7.12	9.13	0.922	5.67	7.05	0.453	2.90
39	7.23	9.75	0.914	5.64	7.71	0.481	3.36
40	7.32	10.45	0.900	5.32	8.50	0.528	4.05
41	7.12	4.62	0.945	7.55	3.48	0.211	2.80
42	6.88	7.50	0.937	7.55	5.51	0.326	3.11
43	6.88	9.88	0.925	7.40	7.35	0.434	3.48
44	7.21	10.60	0.927	7.68	8.25	0.446	3.66
45	7.27	12.47	0.911	7.60	9.95	0.525	3.92
46	7.37	13.71	0.887	6.86	11.39	0.605	6.69

Kuzuryu River, Reporter: Nakamura c.g.s. unit

Run	h_1	U_1	$\nu \cdot 10^2$	$\varepsilon \cdot 10^2$	$R_e \cdot 10^{-5}$	F_d	$f_i \cdot 10^4$
1	120	32.5	0.869	2.06	4.49	0.660	3.94
2	130	20.7	0.861	2.06	3.13	0.404	2.46
3	135	17.5	0.842	2.06	2.81	0.335	45.0
4	175	26.2	0.841	2.06	5.45	0.441	35.0
5	177	19.0	0.841	1.96	4.00	0.326	6.16
6	180	19.1	0.842	2.06	4.08	0.317	15.5
7	272	33.4	0.964	1.96	9.42	0.462	27.2
8	185	34.0	0.928	1.96	6.78	0.570	10.8
9	170	31.8	0.907	2.06	5.96	0.543	6.78
10	182	21.8	0.892	1.57	4.45	0.412	12.8
11	225	25.6	0.907	2.06	6.35	0.380	20.8
12	134	26.3	0.960	1.96	3.67	0.519	10.3
13	148	20.3	0.963	1.96	3.12	0.381	5.10
14	135	19.0	0.950	1.77	2.70	0.393	8.44
15	135	38.8	0.960	1.96	5.46	0.762	29.2
16	185	20.2	0.960	1.96	3.89	0.339	18.6
17	188	31.9	1.063	2.15	5.64	0.507	17.8
18	66	27.5	1.098	2.19	1.65	0.731	4.96
19	124	10.5	1.105	2.18	1.18	0.204	26.8
20	131	8.9	1.105	2.15	1.06	0.170	31.4
21	135	9.0	1.072	2.30	1.13	0.163	3.82
22	130	10.4	1.075	2.23	2.35	0.364	7.04
23	125	23.0	1.075	2.26	2.67	0.437	15.6

Table 1 (continued)

Run	h_1	U_1	$\nu\cdot10^2$	$\varepsilon\cdot10^2$	$R_e\cdot10^{-5}$	F_d	$f_i\cdot10^4$
24	82	31.5	1.140	2.27	2.27	0.738	3.06
25	90	26.5	1.145	2.26	2.08	0.594	6.00
26	110	18.2	1.147	2.24	1.75	0.371	10.9
27	105	16.2	1.147	2.16	1.48	0.344	49.8
28	120	12.5	1.143	2.01	1.31	0.257	26.2
29	125	24.9	1.140	2.25	2.73	0.474	27.8
30	150	23.8	1.137	2.25	3.14	0.414	4.92
31	156	14.0	1.135	2.05	1.92	0.250	19.7
32	195	40.5	1.188	1.96	6.65	0.662	3.22
33	205	35.5	1.179	1.97	6.17	0.564	11.7
34	253	24.2	1.188	1.97	5.15	0.346	20.4
35	324	37.2	1.510	2.30	7.98	0.435	37.8
36	254	31.2	1.425	2.21	5.56	0.420	12.0

Tone River, Reporter: Suga c.g.s. unit

Run	h_1	U_1	ν	ε	$R_e\cdot10^{-5}$	F_d	$f_i\cdot10^5$
1	245	17.0	/	/	4.17	0.315	104
2	305	23.0	/	/	7.02	0.347	66
3	335	24.0	/	/	8.04	0.337	60
4	365	22.0	/	/	8.03	0.602	12
5	385	24.5	/	/	9.43	0.346	38.6
6	410	16.0	/	/	6.56	0.227	89.4
7	240	52.0	/	/	12.5	0.922	2.66
8	300	53.0	/	/	15.9	0.798	4.20
9	315	56.0	/	/	17.6	0.862	1.58
10	330	39.0	/	/	12.9	0.594	7.3
11	350	31.0	/	/	10.9	0.524	9.2
12	140	39.0	/	/	5.46	0.955	2.4
13	230	45.0	/	/	10.4	0.901	3.4
14	260	34.5	/	/	8.97	0.792	6.0
15	290	37.0	/	/	10.7	0.712	10.0
16	320	40.0	/	/	12.8	0.639	12.0
17	350	34.5	/	/	12.1	0.530	18.0
18	50	58.0	/	/	2.9	0.924	5.0
19	240	49.0	/	/	11.8	0.928	2.2
20	290	49.0	/	/	14.2	0.656	13.2
21	330	43.0	/	/	14.2	0.563	14.8
22	355	38.0	/	/	13.5	0.560	11.7
23	380	41.5	/	/	15.8	0.508	11.7
24	160	11.0	/	/	1.76	0.509	84
25	310	11.0	/	/	3.41	0.167	386
26	350	5.0	/	/	1.75	0.124	620
27	410	6.0	/	/	2.46	0.090	688
28	450	6.0	/	/	2.70	0.088	566

Table 1 (continued)

Experiment, Reporter: Suga c.g.s. unit

Run	h_1	U_1	ν	$\varepsilon \cdot 10^2$	$R_e \cdot 10^{-3}$	F_d	$f_i \cdot 10^3$
1	12.75	5.23	/	0.60	6.67	0.605	7.40
2	13.30	5.01	/	0.60	6.67	0.568	6.92
3	13.75	4.85	/	0.60	6.67	0.541	5.94
4	14.10	4.73	/	0.60	6.67	0.521	4.68
5	14.40	4.63	/	0.60	6.67	0.505	4.82
6	14.75	4.52	/	0.60	6.67	0.487	6.62
7	15.15	4.40	/	0.60	6.67	0.468	7.60
8	15.70	4.25	/	0.60	6.67	0.443	11.2
9	16.40	4.07	/	0.60	6.67	0.415	12.5
10	17.25	3.87	/	0.60	6.67	0.385	14.3
11	14.59	9.14	/	0.60	13.3	0.989	0.760
12	16.54	8.06	/	0.60	13.3	0.820	4.88
13	17.49	7.62	/	0.60	13.3	0.754	3.80
14	18.54	7.19	/	0.60	13.3	0.691	7.48
15	21.35	6.25	/	0.60	13.3	0.559	7.50
16	21.85	6.10	/	0.60	13.3	0.540	6.58
17	22.35	5.97	/	0.60	13.3	0.522	6.48
18	22.80	5.85	/	0.60	13.3	0.507	5.90
19	23.20	5.75	/	0.60	13.3	0.494	5.98
20	23.65	5.64	/	0.60	13.3	0.480	6.72
21	24.15	5.52	/	0.60	13.3	0.465	7.08
22	24.65	5.41	/	0.60	13.3	0.451	7.36
23	25.20	5.29	/	0.60	13.3	0.436	7.84
24	25.80	5.17	/	0.60	13.3	0.421	7.82
25	26.40	5.05	/	0.60	13.3	0.406	7.90
26	27.10	4.92	/	0.60	13.3	0.391	8.56
27	28.00	4.76	/	0.60	13.3	0.373	10.9
28	23.20	8.62	/	0.60	20.0	0.740	6.36
29	23.75	8.42	/	0.60	20.0	0.715	4.16
30	24.20	8.26	/	0.60	20.0	0.694	3.28
31	24.60	8.13	/	0.60	20.0	0.678	2.88
32	25.00	8.00	/	0.60	20.0	0.662	3.18
33	25.55	7.83	/	0.60	20.0	0.640	3.56
34	26.20	7.63	/	0.60	20.0	0.617	4.20
35	27.20	7.35	/	0.60	20.0	0.583	4.66
36	11.34	5.88	/	1.0	6.67	0.560	6.6
37	12.09	5.51	/	1.0	6.67	0.509	6.8
38	12.74	5.23	/	1.0	6.67	0.470	6.4
39	13.34	5.00	/	1.0	6.67	0.439	6.2
40	13.79	4.83	/	1.0	6.67	0.418	4.6
41	14.24	4.68	/	1.0	6.67	0.399	6.0
42	14.79	4.51	/	1.0	6.67	0.377	7.0
43	15.39	4.33	/	1.0	6.67	0.355	7.2
44	16.14	4.13	/	1.0	6.67	0.330	7.8
45	14.37	9.28	/	1.0	13.3	0.785	4.12
46	14.97	8.91	/	1.0	13.3	0.739	4.92
47	15.57	8.56	/	1.0	13.3	0.696	4.60
48	16.07	8.30	/	1.0	13.3	0.664	5.82
49	16.67	8.00	/	1.0	13.3	0.629	5.90

Table 1 (continued)

Run	h_1	U_1	ν	$\varepsilon \cdot 10^2$	$R_e \cdot 10^{-3}$	F_d	$f_i \cdot 10^3$
50	17.27	7.72	/	1.0	13.3	0.597	9.47
51	13.10	7.63	/	1.0	10.0	0.694	6.44
52	13.80	7.25	/	1.0	10.0	0.626	6.40
53	14.45	6.92	/	1.0	10.0	0.585	6.02
54	14.95	6.69	/	1.0	10.0	0.555	5.84
55	15.40	6.49	/	1.0	10.0	0.531	5.44
56	15.90	6.29	/	1.0	10.0	0.505	6.18
57	16.40	6.10	/	1.0	10.0	0.484	6.16
58	16.95	5.90	/	1.0	10.0	0.460	7.18
59	17.55	5.70	/	1.0	10.0	0.437	6.66
60	19.54	8.53	/	1.0	16.7	0.620	2.94
61	20.19	8.26	/	1.0	16.7	0.590	4.16
62	20.94	7.96	/	1.0	16.7	0.559	5.14
63	21.74	7.68	/	1.0	16.7	0.528	5.46
64	22.54	7.39	/	1.0	16.7	0.500	5.68
65	23.34	7.14	/	1.0	16.7	0.474	6.14
66	24.24	6.88	/	1.0	16.7	0.448	6.78
67	25.24	6.60	/	1.0	16.7	0.422	7.06
68	26.34	6.33	/	1.0	16.7	0.396	6.98
69	22.00	9.09	/	1.0	20.0	0.622	4.10
70	22.50	8.89	/	1.0	20.0	0.602	4.70
71	23.10	8.66	/	1.0	20.0	0.578	5.32
72	23.70	8.44	/	1.0	20.0	0.557	5.40
73	24.30	8.23	/	1.0	20.0	0.536	5.42
74	24.95	8.02	/	1.0	20.0	0.515	5.76
75	25.65	7.80	/	1.0	20.0	0.494	5.92
76	26.35	7.59	/	1.0	20.0	0.474	5.14
77	27.20	7.35	/	1.0	20.0	0.453	5.56
78	11.59	11.50	/	3.0	13.3	0.632	4.44
79	12.24	10.89	/	3.0	13.3	0.583	4.20
80	12.84	10.38	/	3.0	13.3	0.542	4.74
81	13.44	9.92	/	3.0	13.3	0.507	5.16
82	14.09	9.46	/	3.0	13.3	0.466	6.66
83	14.74	9.05	/	3.0	13.3	0.437	6.74
84	15.49	8.61	/	3.0	13.3	0.405	6.96
85	16.19	8.24	/	3.0	13.3	0.379	6.42
86	16.94	7.87	/	3.0	13.3	0.358	6.26
87	14.20	14.09	/	3.0	20.0	0.699	3.23
88	14.70	13.61	/	3.0	20.0	0.664	3.60
89	15.20	13.16	/	3.0	20.0	0.632	3.92
90	15.70	12.74	/	3.0	20.0	0.602	4.16
91	16.15	12.38	/	3.0	20.0	0.577	3.44
92	16.55	12.09	/	3.0	20.0	0.556	3.48
93	17.00	11.71	/	3.0	20.0	0.534	4.76
94	17.60	11.36	/	3.0	20.0	0.507	5.40
95	13.05	5.10	/	1.0	6.67	0.449	23.0
96	13.45	4.95	/	1.0	6.67	0.434	20.8
97	13.80	4.83	/	1.0	6.67	0.417	18.7
98	14.10	4.76	/	1.0	6.67	0.407	17.3
99	14.10	4.63	/	1.0	6.67	0.391	18.1
100	14.70	4.54	/	1.0	6.67	0.379	16.8

Table 1 (continued)

Run	h_1	U_1	ν	$\varepsilon \cdot 10^2$	$R_e \cdot 10^{-3}$	F_d	$f_i \cdot 10^3$
101	14.95	4.45	/	1.0	6.67	0.370	15.4
102	15.20	4.39	/	1.0	6.67	0.361	15.5
103	15.45	4.31	/	1.0	6.67	0.352	17.1
104	15.75	4.23	/	1.0	6.67	0.342	20.0
105	16.10	4.14	/	1.0	6.67	0.332	21.2
106	16.45	4.05	/	1.0	6.67	0.321	21.6
107	16.85	3.95	/	1.0	6.67	0.310	23.8
108	20.70	6.44	/	1.0	13.3	0.455	8.12
109	21.00	6.35	/	1.0	13.3	0.445	5.94
110	21.20	6.29	/	1.0	13.3	0.438	4.82
111	21.40	6.23	/	1.0	13.3	0.432	4.86
112	21.60	6.17	/	1.0	13.3	0.427	5.52
113	21.85	6.10	/	1.0	13.3	0.420	6.18
114	22.10	6.03	/	1.0	13.3	0.412	6.86
115	22.40	5.95	/	1.0	13.3	0.404	7.58
116	22.70	5.87	/	1.0	13.3	0.396	7.60
117	23.00	5.80	/	1.0	13.3	0.389	7.60
118	23.30	5.72	/	1.0	13.3	0.381	7.62
119	23.60	5.65	/	1.0	13.3	0.373	8.26
120	23.95	5.57	/	1.0	13.3	0.365	8.84
121	24.30	5.49	/	1.0	13.3	0.358	9.30
122	24.70	5.40	/	1.0	13.3	0.349	10.3
123	25.15	5.30	/	1.0	13.3	0.339	11.8
124	13.60	6.62	/	1.0	3.38	0.576	11.5
125	14.00	6.43	/	1.0	3.38	0.551	10.2
126	14.35	6.27	/	1.0	3.38	0.532	9.18
127	14.65	6.14	/	1.0	3.38	0.515	8.06
128	14.90	6.04	/	1.0	3.38	0.502	7.46
129	15.15	5.94	/	1.0	3.38	0.490	7.56
130	15.40	5.84	/	1.0	3.38	0.479	7.62
131	15.65	5.75	/	1.0	3.38	0.467	7.66
132	15.90	5.66	/	1.0	3.38	0.456	8.42
133	16.20	5.56	/	1.0	3.38	0.443	10.7
134	16.60	5.42	/	1.0	3.38	0.428	11.9
135	17.00	5.29	/	1.0	3.38	0.412	11.4
136	17.40	5.17	/	1.0	3.38	0.397	12.0
137	17.57	3.79	/	0.6	6.67	0.374	23.4
138	17.97	3.71	/	0.6	6.67	0.362	19.2
139	18.37	3.63	/	0.6	6.67	0.351	20.1
140	18.77	3.55	/	0.6	6.67	0.339	20.8
141	19.17	3.48	/	0.6	6.67	0.329	21.4
142	19.57	3.41	/	0.6	6.67	0.318	22.1
143	19.97	3.34	/	0.6	6.67	0.308	22.6
144	20.37	3.27	/	0.6	6.67	0.300	20.0
145	20.67	3.23	/	0.6	6.67	0.293	17.3
146	20.97	3.18	/	0.6	6.67	0.286	17.5
147	21.27	3.13	/	0.6	6.67	0.281	17.8
148	21.57	3.09	/	0.6	6.67	0.276	17.8
149	21.87	3.05	/	0.6	6.67	0.270	19.4
150	22.17	3.02	/	0.6	6.67	0.265	19.4
151	22.47	2.99	/	0.6	6.67	0.261	17.2